Adhesion phenomena in ferrofluids

José A. Miranda* and Rafael M. Oliveira
Laboratório de Física Teórica e Computacional, Departamento de Física, Universidade Federal de Pernambuco, Recife, Pernambuco 50670-901, Brazil

David P. Jackson
Department of Physics and Astronomy, Dickinson College, Carlisle, Pennsylvania 17013, USA
(Received 4 March 2004; published 21 September 2004)

One efficient way of determining the bond strength of adhesives is to measure the force or the work required to separate two surfaces bonded by a thin adhesive film. We consider the case in which the thin film is not a conventional adhesive material but a high viscosity ferrofluid confined between two narrowly spaced parallel flat plates subjected to an external magnetic field. Our theoretical results demonstrate that both the peak adhesive force and the separation energy are significantly influenced by the action and symmetry properties of the applied field. Specifically, we show that the adhesive strength of a ferrofluid is reduced if the applied magnetic field is perpendicular to the plates or if the applied field is in plane and exhibits azimuthal symmetry. Conversely, the adhesive strength can be either enhanced or reduced if the applied field is in plane and is directed radially outward. This establishes an interesting connection between adhesion and ferrohydrodynamic phenomena, allowing the control of important adhesive properties by magnetic means.

DOI: 10.1103/PhysRevE.70.036311 PACS number(s): 47.65.+a, 75.50.Mm, 68.35.Np

I. INTRODUCTION

The study of adhesive materials is vastly multidisciplinary and its basic scientific research involves a broad spectrum of areas ranging from interfacial science and rheology to pattern formation and chemistry [1,2]. On the practical side, the phenomenon of adhesion is part of our everyday lives, and adhesive tape industries are among the most active and profitable [3].

One key aspect on both scientific and practical levels is to precisely evaluate, characterize, and hopefully *control*, the bond strength of adhesives. One efficient and relatively simple way to study important adhesive properties is provided by the so-called probe-tack test [4,5], which measures the force required to separate two surfaces bonded by a thin adhesive film. The result of such a test is a force-distance curve, that describes the behavior of the adhesive film under tension. Good adhesives typically present highly nonlinear force-distance curves, in which the force increases sharply, reaches a maximum value, and then drops abruptly, defining a plateau, before it eventually vanishes. From these curves the separation energy (work done during the entire separation process), as well as the peak adhesive force, can be determined.

Recently, several groups began investigating the fundamentals of adhesion in viscous liquids [6–10]. By dealing with simpler Newtonian and non-Newtonian fluids, these interesting studies tried to gain more insight into the relation between the complicated rheological properties of conventional adhesives and the force-distance curves. Some noteworthy findings include the appearance of a cavitation-induced force plateau for high separation velocities in very viscous fluids [7], and the important verification of a modest influence of fingering instabilities on the shape of the curves [8]. As systematically proposed by Francis and Horn [6], all these works [6–10] take into account the significant dependence of the force-distance curves on the compliance of the measurement apparatus.

In this paper we consider the case in which the fluid used in the adhesion probe-tack test is a magnetic liquid called a *ferrofluid*. The field of ferrofluid research is also highly interdisciplinary, bringing physicists, chemists, engineers, and even physicians together [11,12]. Ferrofluids are colloidal suspensions of nanometer-sized magnetic particles suspended in a nonmagnetic carrier fluid. These fluids behave superparamagnetically and can easily be manipulated with external magnetic fields that can act to either stabilize or destabilize the fluid interface. As a result of the ferrofluid interaction with the external field in confined geometries, the usual viscous fingering instability (Saffman-Taylor instability [13]) is supplemented by a magnetic fluid instability [11,12], resulting in a variety of interesting interfacial behaviors. Depending on the applied field direction, one observes highly branched, labyrinthine structures [14–17], patterns showing an ordered line of peaks [18], or even the suppression of viscosity-driven [19] and centrifugally induced [20,21] interfacial instabilities in thin ferrofluid films.

We stress that although these ferrofluids are viscous and magnetic, they are not, rigorously speaking, "true" (non-Newtonian) adhesives. However, in certain situations these fluids have properties that are quite similar to regular adhesives. Here we show that, in contrast to conventional adhesive materials, the adhesive properties of a ferrofluid can be enhanced or reduced by varying the intensity of an externally applied magnetic field. This effect could be used to design versatile adhesive materials with highly flexible properties that vary with magnetic field, in which the bonding between surfaces could be manipulated in a nondestrucitve way. The

*Email address: jme@df.ufpe.br

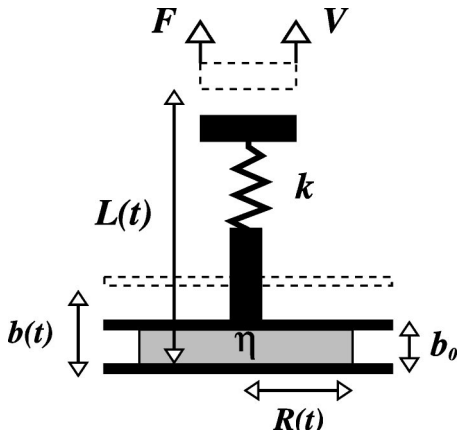

FIG. 1. Schematic diagram for the plate-plate geometry and lifting apparatus of the adhesion measurement system with ferrofluids.

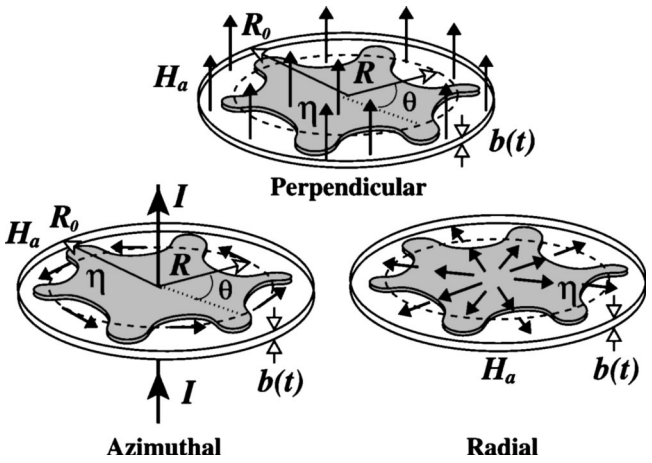

FIG. 2. Schematic diagrams for the different magnetic field configurations considered in this paper.

simplicity and potential usefulness of such a regulatory mechanism could be of great value in many applications.

This paper is organized as follows: Sec. II formulates our theoretical approach and derives the adhesion force between two flat plates due to the presence of a ferrofluid subjected to an external magnetic field. We study three different magnetic field configurations: (i) *perpendicular*, when a uniform field is normal to the plates of the apparatus, (ii) *azimuthal*, for an in-plane field produced by a long current-carrying wire oriented perpendicular to the plates, and (iii) *radial*, for a cylindrically radial magnetic field pointing away from the cylinder's symmetry axis and decreasing linearly with radial distance. Initially, the probe-tack apparatus is considered to be perfectly rigid, and we focus on the derivation of the adhesive force under the influence of magnetic interactions. Section III discusses the effects of the three magnetic field arrangements on the force-distance curves for the ferrofluid sample. We find that the adhesive strength of the ferrofluid is decreased in the perpendicular and azimuthal configurations and can be either increased or decreased in the radial case. The influence of the magnetic forces on the separation energy is also investigated. Section IV studies the combined effects of the apparatus' intrinsic compliance and the magnetic forces, and discusses their role in determining the force-distance profiles. Our chief conclusions and perspectives are summarized in Sec. V. Last, an alternative method for determining the magnetic forces is discussed in the Appendix.

II. ADHESION FORCE: DARCY'S LAW FORMULATION

Figure 1 sketches the geometry of the system under study. We consider a Newtonian, incompressible ferrofluid of high viscosity η located between two narrowly spaced circular, flat plates. The outer fluid is nonmagnetic, and of negligible viscosity. As in Refs. [6–10] we consider that the apparatus has a spring constant denoted by k. One end of the lifting apparatus moves at a specified constant velocity V, subjecting the upper plate to a pulling force F. The lower plate is held fixed at $z=0$, where the z axis points in the direction perpendicular to the plates. The initial plate-plate distance is represented by b_0 and the initial ferrofluid radius by R_0. At a given time t the plate spacing is $b=b(t)$, while the deformation due to the stretching of the apparatus is $L-b$, where $L=b_0+Vt$. We stress that due to the compliance of the measurement apparatus, the actual plate spacing b is not necessarily equivalent to L. Of course, in the case of a completely rigid apparatus we have $b=L$ and $\dot{b}=V$, where $\dot{b}=db/dt$. The perpendicular, azimuthal, and radial magnetic field configurations are schematically illustrated in Fig. 2.

Our initial task is to calculate the pulling force F as a function of displacement L, taking into account both hydrodynamic and magnetic contributions. We follow Derks *et al.* [8] and derive F assuming that the ferrofluid interface remains circular during the entire lifting process, with time-dependent radius defined as $R=R(t)$. This approach is justified in Ref. [8], where it has been found that experiments showing strong fingering instabilities are very well described by theoretical force-distance curves which assume an exact circularity of the evolving interface. In the perpendicular magnetic field configuration conservation of ferrofluid volume leads to the useful relation $R^2b=R_0^2b_0$. This expression can be trivially modified in order to account for the radius of the current-carrying wire or the cylindrical magnet in the azimuthal and radial field cases.

To study the hydrodynamics of the system, the usual Navier-Stokes equation is modified through the inclusion of terms representing the magnetic effects. We follow the standard approximations used by Rosensweig [11] and others [12,14–16] and assume that the ferrofluid is magnetized such that its magnetization $\mathbf{M}$ is collinear with the applied field $\mathbf{H}_a$. When this is the case, the magnetic body force is given by $\mu_0 M \nabla H$, where μ_0 is the magnetic permeability of free space and H is the *local* magnetic field. The local magnetic field can include contributions from the applied field as well as the demagnetizing field. We consider only the lowest order effect of the magnetic interactions that would result in fluid motion. Thus, in the azimuthal and radial situations, we consider only the applied field in determining the magnetization. However, in the perpendicular situation, we include the demagnetizing field produced by the uniform magnetization resulting from the applied field.

For the quasi-two-dimensional plate-plate geometry, we employ the lubrication approximation and reduce the three-dimensional flow to an equivalent two-dimensional flow $\mathbf{U}(r,\theta)$ by averaging over the direction perpendicular to the plates (z axis), where (r,θ) denote polar coordinates. Using no-slip boundary conditions and neglecting inertial terms, one derives a modified Darcy's law as [16,22]

$$\mathbf{U} = -\frac{b^2}{12\eta}\boldsymbol{\nabla}\Pi_j. \tag{1}$$

The generalized pressure $\Pi_j = p - \Psi_j$ in Eq. (1) contains both the hydrodynamic pressure p and a magnetic pressure represented by a scalar potential Ψ_j. The subscript $j=1,2,3$ indicates the perpendicular, azimuthal, and radial magnetic field configurations, respectively.

We can exploit the irrotational nature of the flow to obtain the two-dimensional flow field by z averaging the full three-dimensional incompressibility condition $\boldsymbol{\nabla}\cdot\boldsymbol{v}=0$. This yields $\mathbf{U}(r) = -(\dot{b}r/2b)\hat{\mathbf{e}}_r$, where $\hat{\mathbf{e}}_r$ is a unit vector in the radial direction. This allows us to integrate Eq. (1) to obtain the pressure field

$$\Pi_j(r) = \frac{3\eta\dot{b}}{b^3}(r^2 - R^2) + \Pi_j(R), \tag{2}$$

where $\Pi_j(R)$ is the value of the generalized pressure at the ferrofluid droplet boundary. To determine $\Pi_j(R)$ we use the facts that $\Psi_j = 0$ in the nonmagnetic fluid and the pressure jump at the interface of a magnetic fluid given by [11,12]

$$\Delta p = \sigma\kappa - \frac{1}{2}\mu_0 M_n^2. \tag{3}$$

Here, σ is the surface tension, κ is the curvature of the interface, and M_n represents the normal component of the magnetization at the interface. In the present case, M_n is given by the radial component evaluated at $r=R$, namely, $M_n = M_r(R)$. These boundary conditions result in a pressure field given by

$$\Pi_j(r) = \frac{3\eta\dot{b}}{b^3}(r^2 - R^2) + p_0 - \Psi_j(R) - \frac{1}{2}\mu_0 M_{jr}^2(R), \tag{4}$$

where p_0 denotes the atmospheric pressure outside the ferrofluid droplet. As is common in this type of adhesion phenomena [6–10], we have neglected the surface tension term in Eq. (4).

In the nonmagnetic case, the inward viscous flow induced by traction is accompanied by a pressure gradient pointing outward. Therefore in the absence of an applied magnetic field the border of the ferrofluid droplet is at atmospheric pressure p_0 while the interior of the sample is at a lower pressure. From Eq. (4) we see that the purely viscous, nonmagnetic contribution to the pressure in the sample is negative. In other words, when the upper plate is lifted, the pressure gradient causes an inward viscous shearing flow in the plane of the adhesive film, producing a downward adhesive force normal to the upper plate. When a magnetic field is applied, the magnetic contributions in Eq. (4) can modify this scenario significantly. In fact, as we now show, additional magnetic terms come into play when calculating the adhesion force.

Since it is the generalized pressure Π_j that results in fluid motion according to Eq. (1), the force exerted by the lifting machine on the upper plate is calculated by integrating the generalized pressure difference above and below the upper plate, taking into account the pressure jump condition (3) across the magnetic fluid surface in contact with the upper plate. The net force of separation (adhesion force) is then given by

$$F_j = \int d\mathcal{A}\left\{\frac{3\eta\dot{b}}{b^3}(R^2 - r^2) + [\Psi_j(R) - \Psi_j(r)] + \frac{1}{2}\mu_0[M_{jr}^2(R) - M_{jz}^2(r)]\right\}, \tag{5}$$

where the integration is carried out over the cross sectional area of the ferrofluid drop $\mathcal{A}$. In the perpendicular case, this is simply a circle of radius R. But in the azimuthal and radial situations, this is an annulus of outer radius R and inner radius a. The term $M_{jz}^2(r)$ denotes the normal component of the magnetization evaluated at the boundary $z=b$. An alternative way of calculating the magnetic terms appearing in the adhesion force Eq. (5) is presented and discussed in the Appendix.

We can gain some physical insight into the adhesion force equation simply by looking at the sign of the magnetic terms. Positive magnetic terms in Eq. (5) lead to increased adhesion while negative terms lead to decreased adhesion. In particular, any radial magnetization at the boundary of the domain will tend to increase adhesion while magnetization normal to the plates will tend to decrease adhesion. This can be understood qualitatively by noting that the effect of the normal component of the magnetization at the fluid interface $r=R$ is to "push" outward on the interface. Thus magnetization that pushes outward at the boundary of the domain leads to the fluid attempting to "spread out" in the plane of the sample. This results in a downward force on the upper plate and an increase in adhesion. Conversely, magnetization that pushes upward on the upper surface $z=b$ will exert an upward force on the plate, resulting in decreased adhesion. The effect of the other magnetic terms in Eq. (5) will depend on the form of the scalar potential.

Equation (5) is one of the central results of this work. The remainder of this paper looks into the details of how the magnetic effects alter the adhesion force for three different magnetic field configurations.

A. Perpendicular magnetic field

First, we consider the perpendicular field case ($j=1$) in which a uniform magnetic field $\mathbf{H}_a = H_0\hat{\mathbf{e}}_z$ is applied normal to the plates. This situation was studied in Refs. [15,23] by assuming the ferrofluid has a uniform magnetization $M_0 = M(H_0)$. Here, $M(H)$ gives the (possibly nonlinear) relationship between the magnetization and the applied field. This configuration is then equivalent to a uniformly charged

parallel-plate capacitor and a scalar potential can be written in a number of equivalent forms [16]. However, in contrast to the situation studied in Refs. [15,16,23], which only required the magnetic pressure at the *interface* of a fingered droplet, we are interested in calculating Ψ_1 for an *arbitrary point* $\mathbf{r}$ of a circular magnetic domain ($0 \leqslant r \leqslant R$). In particular, since we are interested in points *within* as well as *on* the domain boundary, it is essential to choose a form for Ψ_1 that is *continuous* at the boundary. If we describe the ferrofluid boundary by a simple closed curve C parametrized by arclength s, then a convenient way of writing the scalar potential is (see Ref. [16])

$$\Psi_1 = \frac{\mu_0 M^2}{2\pi b}\left\{ \oint_C ds' \hat{\mathbf{D}} \times \hat{\mathbf{t}}(s') + \oint_C dx' \ln\left[(y-y') + \sqrt{D^2+b^2}\right]\right\}, \tag{6}$$

where $x=x(s)$, $x'=x(s')$, etc., $\hat{\mathbf{t}}(s')$ is the unit tangent vector at arclength s', and $\hat{\mathbf{D}}=\mathbf{D}/D$ is the unit difference vector pointing from the point $\mathbf{r}=(x,y)$ to the point $\mathbf{r}'=(x',y')$.

Unfortunately, even though we assume the ferrofluid sample maintains a circular shape during the lifting of the upper plate, the evaluation of Eq. (6) for arbitrary points located inside the sample does not result in a simple closed-form expression. Substituting Eq. (6) into Eq. (5) results in a *dimensionless* force

$$F_1 = \frac{\dot{b}}{b^5} + N_B^{\perp}\left\{ \frac{2}{R_0^2}\int_0^R \mathcal{I}(r) r dr - \left(\frac{b_0}{b}\right)\left[\mathcal{I}(R) + \frac{\pi}{2}\right]\right\}, \tag{7}$$

where

$$\mathcal{I}(r) = \int_0^{\pi/2}\left(\frac{\zeta Q + P^2 \sin^2\omega}{\sqrt{Q^2+P^2\sin^2\omega}}\right)d\omega + \frac{1}{2}\int_0^{\pi}\ln\left[\sqrt{1+Q^2+P^2\sin^2\omega} - \frac{1}{2}\zeta \sin 2\omega\right] \times \zeta \sin 2\omega \, d\omega, \tag{8}$$

$\zeta=2R/b$, $Q=(R-r)/b$, $P^2=4rR/b^2$, and $N_B^{\perp}=\mu_0 M^2 R_0^2/k\delta$ is the magnetic Bond number for the perpendicular magnetic field configuration. Similar to what is done in Refs. [6,8,10], in Eq. (7) lengths have been re-scaled by $\delta=(3\pi\eta R_0^4 b_0^2 V/2k)^{1/6}$ and velocities by V. It is worth mentioning again that since we are dealing with the noncompliant situation, we have $b=L$ and hence $\dot{b}=1$. Equation (7) shows $\dot{b}$ explicitly in anticipation of our analysis of the compliant apparatus situation.

B. Azimuthal magnetic field

For the azimuthal field case ($j=2$) we consider a long straight current-carrying wire that is perpendicular to (coaxial with) the plates (see Fig. 2). This may present an experimental challenge because the hole necessary for the wire could result in leakage. The magnetic field produced by this wire is $\mathbf{H}_a = I/(2\pi r)\hat{\mathbf{e}}_\theta = (H_0 a/r)\hat{\mathbf{e}}_\theta$, where I represents the electric current, a is the radius of the current-carrying wire, and $\hat{\mathbf{e}}_\theta$ is a unit vector in the azimuthal direction. The magnetization is collinear with the magnetic field and is written $\mathbf{M}=(M_0 a/r)\hat{\mathbf{e}}_\theta$, where $M_0=M(H_0)$. Here again, $M(H)$ gives the (possibly nonlinear) relationship between the magnetization and the applied field. In this case, the scalar potential can be simply written as [20]

$$\Psi_2(r) = \frac{\mu_0 M_0 H_0 a^2}{2r^2}. \tag{9}$$

We note that the magnetization in this configuration is everywhere tangential to the interface, and also to the upper surface of the ferrofluid sample. Thus there are no "surface" contributions to the adhesion force. Furthermore, we note that $[\Psi_2(R)-\Psi_2(r)]$ will always be negative so that the magnetic contribution in the azimuthal case tends to reduce the bond strength of the ferrofluid. This makes good physical sense because the radial gradient results in a magnetic force directed radially inward leading to an increased pressure that pushes upward on the upper surface.

Under such circumstances, the evaluation of Eq. (5) for the azimuthal field case leads to the *dimensionless* force

$$F_2 = \frac{\dot{b}}{b^5}\left(\frac{\gamma-1}{\gamma}\right)^2 - N_B^{\mathrm{azi}}\left\{\ln\left[1+(\gamma-1)\frac{b_0}{b}\right] - \left[\frac{(\gamma-1)}{\frac{b}{b_0}+(\gamma-1)}\right]\right\}, \tag{10}$$

where $\gamma=(R_0/a)^2$ and $N_B^{\mathrm{azi}}=(\pi\mu_0 M_0 H_0 a^2)/(2k\delta)$ is a magnetic Bond number for the azimuthal magnetic field configuration. In the case of a linear relationship $M=\chi H$, the Bond number can be written $N_B^{\mathrm{azi}}=(\mu_0\chi I^2)/(8\pi k\delta)$. As in the perpendicular field case, lengths and velocities in Eq. (10) have been re-scaled by δ and V, respectively, and $\dot{b}=1$.

C. Radial magnetic field

Last, we consider a cylindrically radial magnetic field configuration ($j=3$) [24–26] such that $\mathbf{H}_a=(H_0 a/r)\hat{\mathbf{e}}_r$. The experimental conditions required to obtain such a radial magnetic field are discussed in Ref. [24]. Roughly speaking, the radial field is produced by shaping the poles of a permanent magnet into concentric cylinders. As before, we assume the magnetization is collinear with the applied field so that $\mathbf{M}=(M_0 a/r)\hat{\mathbf{e}}_r$, where $M_0=M(H_0)$. In this case, the scalar potential can be written as

$$\Psi_3(r) = \frac{\mu_0 M_0 H_0 a^2}{2r^2}. \tag{11}$$

Note that the scalar potential in this situation is exactly the same as in the azimuthal field configuration. Thus we already know that the force resulting from this potential will tend to decrease the adhesion force. However, unlike the azimuthal case, the radial magnetization will lead to a "surface" force

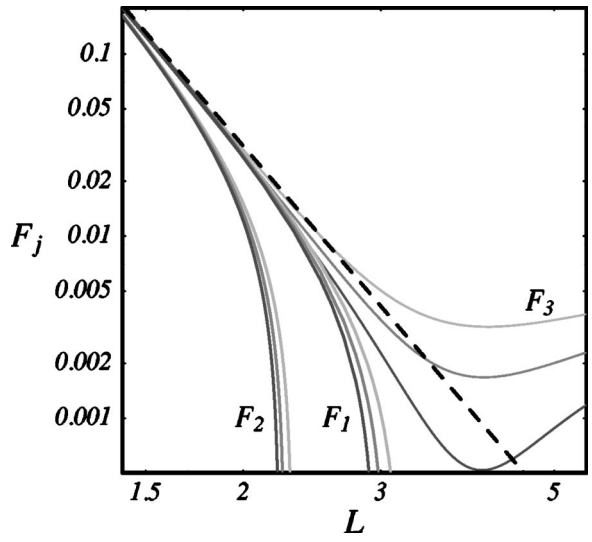

FIG. 3. Pulling force F_j as a function of L for the purely rigid case described by Eqs. (7), (10), and (12). The dashed line shows the nonmagnetic case and the solid curves show the magnetic situations with $N_B^{\perp}=5.0\times10^{-2}$, $N_B^{\mathrm{azi}}=5.0\times10^{-3}$, and $N_B^{\mathrm{rad}}=5.0\times10^{-3}$. The solid curves are plotted in hues of gray for $b_0=1.2$ (light), $b_0=1.7$ (medium), and $b_0=2.2$ (dark).

term that will tend to *increase* adhesion. Under such circumstances, the evaluation of Eq. (5) for the radial field case leads to a *dimensionless* force

$$F_3=\frac{\dot{b}}{b^5}\left(\frac{\gamma-1}{\gamma}\right)^2-N_B^{\mathrm{rad}}\left\{\ln\left[1+(\gamma-1)\frac{b_0}{b}\right]-\left(1+\frac{M_0}{H_0}\right)\times\left[\frac{(\gamma-1)}{\frac{b}{b_0}+(\gamma-1)}\right]\right\},\tag{12}$$

where $\gamma=(R_0/a)^2$ and $N_B^{\mathrm{rad}}=(\pi\mu_0 M_0 H_0 a^2)/(2k\delta)$ is a magnetic Bond number for the radial magnetic field configuration. In the case of a linear relationship $M=\chi H$, the Bond number can be written $N_B^{\mathrm{rad}}=(\pi\mu_0\chi H_0^2)/(2k\delta)$. As in the other cases, lengths and velocities in Eq. (12) have been re-scaled by δ and V, respectively, and $\dot{b}=1$.

We note in passing that by taking the limit $a\to0$ and eliminating the magnetic terms (by simply dropping the terms involving the magnetic Bond numbers), all three force equations (7), (10), and (12) reduce to the equivalent expression derived in Ref. [8] for nonmagnetic viscous fluids. As we will see in the remaining sections, the magnetic terms appearing in these force expressions enrich the physics involved considerably, establishing an interesting link between adhesion and magnetic phenomena.

III. NONCOMPLIANT APPARATUS CASE

Before turning our attention to the complete force-distance curves including compliance and magnetic effects, let us analyze Eqs. (7), (10), and (12) in greater detail and explore the relevant aspects coming from the magnetic contribution. Figure 3 is a log-log plot that depicts the pulling force F_j for the rigid apparatus case where $b=L$ (and $\dot{b}=1$). Along with the usual nonmagnetic case (dashed line), we have plotted three sets of curves: (1) the perpendicular case given by Eq. (7) with $N_B^{\perp}=5.0\times10^{-2}$, (2) the azimuthal case given by Eq. (10) with $N_B^{\mathrm{azi}}=5.0\times10^{-3}$, and (3) the radial case given by Eq. (12) with $N_B^{\mathrm{rad}}=5.0\times10^{-3}$. The shading represents different initial plate spacings given by $b_0=1.2$ (light gray), $b_0=1.7$ (medium gray), and $b_0=2.2$ (dark gray). In addition, we have set the parameters $R_0=100$, $\gamma=100$, and $M_0/H_0=3.0$.

It is clear from Fig. 3 that the presence of magnetic forces can alter the adhesion force in markedly different ways. For relatively small separation L the curves are quite similar to the nonmagnetic case for all magnetic field configurations. However, as L is increased, the magnetic cases depart more and more from the nonmagnetic situation. Eventually, each magnetic case is split further depending on the initial plate spacing b_0.

We note that the behavior of the perpendicular and azimuthal field configurations is qualitatively similar. In both cases, the adhesion force is decreased (compared to a nonmagnetic liquid) throughout the entire range of L. The azimuthal case leads to a much more dramatic decrease than the perpendicular case but the perpendicular case appears to be more sensitive to the initial plate spacing.

Interestingly, the adhesion force in the perpendicular and azimuthal magnetic field configurations becomes negative and then falls asymptotically to zero as L increases. This is in stark contrast to a nonmagnetic liquid in which the adhesion force is always positive and drops smoothly to zero as $1/L^5$. Thus, in these two magnetic field configurations, this force will cease to be an *adhesion* force and will instead become a sort of *separation* force. Thus, instead of pulling on the plates, one would need to start pushing to keep the plate velocity constant. Thus it may be possible to create a ferrofluid adhesive such that the adhesive force can be completely eliminated simply by bringing a small hand magnet up close.

The situation is even more interesting in the radial field configuration. Here, we have the possibility of increased or decreased adhesion compared to a nonmagnetic liquid. This configuration is also much more sensitive to the initial plate spacing than the other configurations, with smaller initial plate spacings leading to more increased adhesion. However, unlike the perpendicular and azimuthal cases, the adhesion in the radial case may or may not become negative as L increases. This depends on the value of the parameter M_0/H_0 (the magnetic susceptibility χ in the linear case). In addition, by taking the large b limit of Eq. (12), we see that $F_3\sim1/L$ so that for large enough L, the adhesion force in the radial case will always end up larger than the adhesion force in the nonmagnetic case. Thus, in the radial case, there are two possibilities. Either the adhesion force remains an adhesion force throughout the entire plate separation process, or the adhesion force first becomes a separation force and then returns to being an adhesion force as the plates are separated.

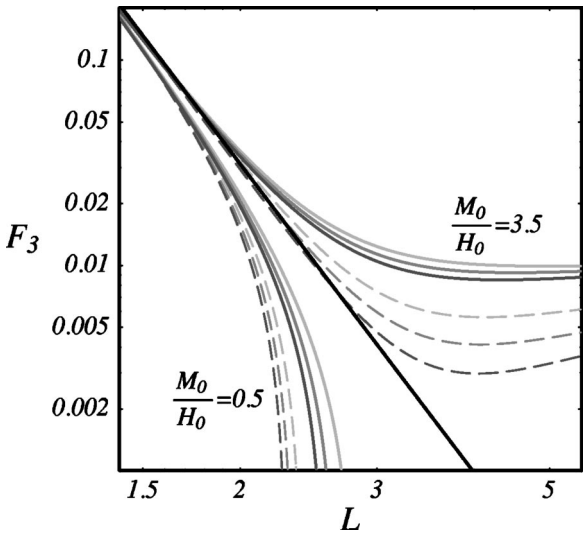

FIG. 4. Pulling force F_3 for radial magnetic field case described by Eq. (12). The solid black line denotes a nonmagnetic fluid while the dashed (solid) gray curves have $\gamma=100$ ($\gamma=25$). The curves with $M_0/H_0=0.5$ lead to decreased adhesion while those with $M_0/H_0=3.5$ lead to increased adhesion for small plate spacings.

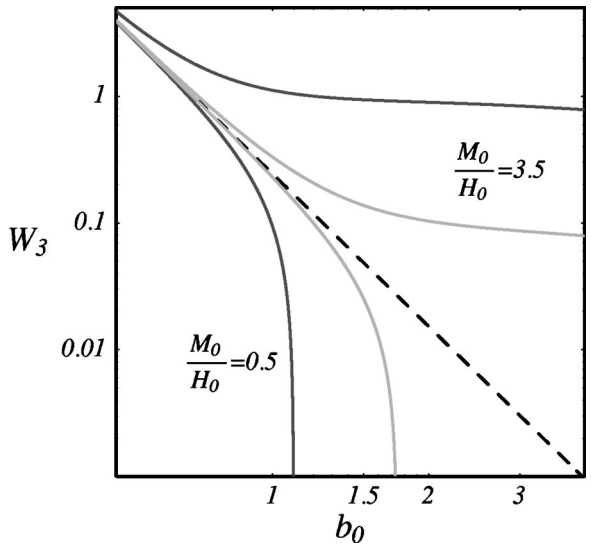

FIG. 5. Work of separation W_3 as a function of b_0 for the purely rigid case for a nonmagnetic (dashed) and a magnetic liquid in the radial field configuration (solid). Two values of M_0/H_0 are used and the light (dark) gray curves have $N_B^{\mathrm{rad}}=5.0\times10^{-4}$ ($N_B^{\mathrm{rad}}=5.0\times10^{-3}$).

Figure 4 examines the radial situation further by varying both γ and M_0/H_0. As in Fig. 3, $N_B^{\mathrm{rad}}=5.0\times10^{-3}$ and the shading represents the same initial plate spacings $b_0=1.2$ (light gray), $b_0=1.7$ (medium gray), and $b_0=2.2$ (dark gray). The solid black line is the nonmagnetic case and the dashed (solid) curves have $\gamma=100$ ($\gamma=25$) and M_0/H_0 is either 0.5 or 3.5 as labeled in the figure. The most obvious feature of Fig. 4 is that the value of M_0/H_0 determines whether adhesion is increased or decreased for small plate spacings. Of course, for large enough plate spacing, we have already seen that adhesion will be increased relative to a nonmagnetic liquid. As a practical matter, there is a point at which the fluid film will rupture or the lubrication approximation will no longer be valid. Selecting M_0/H_0 can therefore effectively result in a magnetic liquid that either increases or decreases adhesion throughout the useful range of b.

Another relevant physical quantity of interest is the work of separation given by

$$W_j=\int_{b_0}^{L_f}F_j\,dL. \tag{13}$$

For a nonmagnetic liquid and for the perpendicular and azimuthal situations, the upper limit of integration can safely be taken to be $L_f=\infty$ with no problems. However, in the radial magnetic field configuration, the large L force varies as $1/L$ so the work of separation diverges logarithmically. This causes some difficulty in trying to calculate the work of separation as there is no obvious termination point for this integral. We follow the approach adopted in Ref. [6], and integrate Eq. (13) to a finite end point. Consistently with the restrictions imposed by the lubrication approximation, we take $L_f=\beta$, where $\beta\gg b_0$. Using $\beta=100$, Fig. 5 illustrates how the work of separation W_3 varies with initial plate spacing b_0 for a nonmagnetic liquid (dashed) and for a magnetic liquid in the radial field configuration (solid). As in Fig. 4, we take M_0/H_0 as either 0.5 or 3.5 and use two different magnetic Bond numbers, $N_B^{\mathrm{rad}}=5.0\times10^{-4}$ (light gray) and $N_B^{\mathrm{rad}}=5.0\times10^{-3}$ (dark gray). The results for the azimuthal and perpendicular cases are qualitatively similar to the $M_0/H_0=0.5$ results in the radial case and are therefore not shown.

IV. COMPLIANT APPARATUS CASE

As briefly discussed at the beginning of this work, typical force-distance curves increase sharply during the initial stages of the plate separation process. This effect is not described by the ferrohydrodynamic forces within the ferrofluid, but is a result of the elasticity of the apparatus [6,8]. Now we examine the complete form of the force-distance curves, including the magnetic properties of the ferrofluid and the intrinsic flexibility of the lifting machine. To accomplish this, we adapt a method originally developed by Francis and Horn [6] for their sphere-plate geometry with nonmagnetic fluids.

It is assumed that, during the entire separation process, there is a perfect balance between the viscous, ferrohydrodynamic force and the spring restoring force $L-b$ which results from the deflection of the apparatus. By equating Eqs. (7), (10), and (12), to $L-b$, we obtain nonlinear first order differential equations for $b=b(t)$. Then, using the relation $L=b_0+t$ we can write $\dot{b}=db/dL$ so that

$$F_j(b,b')=L-b, \tag{14}$$

where the prime denotes differentiation with respect to L. We utilize differential equations (14) to obtain the complete force-distance profiles. We solve them numerically for $b(L)$ and find the force curves from $F_j=L-b(L)$.

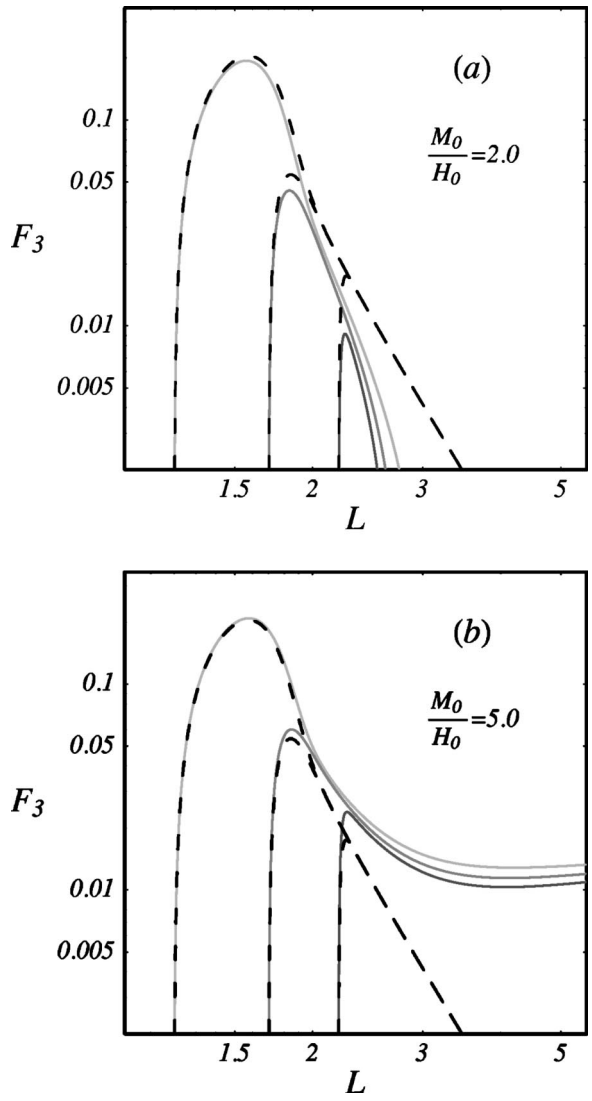

FIG. 6. Force $F_3=L-b(L)$ as a function of displacement L for the flexible apparatus case for three initial plate spacings b_0. The curves are obtained by numerically solving Eq. (14) with F_j given by Eq. (12). The black dashed curves are for zero magnetic field and the gray solid curves have $N_B^{\mathrm{rad}}=5.0\times10^{-3}$, $\gamma=100$, and $b_0=1.2$ (light), $b_0=1.7$ (medium), and $b_0=2.2$ (dark).

Figure 6 presents the complete force-distance curves for thin layers of ferrofluid obtained by numerically solving Eq. (14) with F_3 given by Eq. (12). It compares the curves in the absence of magnetic field (black dashed curves) with those calculated for nonzero applied field (gray solid curves). We use $N_B^{\mathrm{rad}}=5.0\times10^{-3}$, $\gamma=100$, and two values of M_0/H_0. As in Figs. 3 and 4, the gray hues indicate the initial plate spacing with $b_0=1.2$ (light gray), $b_0=1.7$ (medium gray), and $b_0=2.2$ (dark gray). The perpendicular and azimuthal field results are again qualitatively similar to the radial case with $M_0/H_0=2.0$ and are therefore not shown.

By inspecting Figs. 6(a) and 6(b), we conclude that during the beginning of the plate separation process the system is dominated by the elastic force regardless of the nature (perpendicular, azimuthal, or radial) of the applied magnetic field. We also note that the peak adhesive force decreases considerably in the perpendicular and azimuthal cases but can be either decreased or increased in the radial case depending on M_0/H_0. In all field configurations, this increase or decrease in the peak force is more pronounced for larger b_0.

Towards the end of the lifting process the contribution from the ferrohydrodynamic force becomes much more important. One can see from Figs. 6(a) and 6(b) that the behavior of the force can be "controlled" in some sense depending on the type of ferrofluid and the field configuration. When the applied field is zero, there is no magnetic force and all cases converge to the same $1/L^5$ behavior that was seen in Fig. 3. In the perpendicular and azimuthal magnetic field cases, the magnetic forces decrease adhesion and the force curves all drop off more rapidly than in the nonmagnetic case, separated slightly based on the initial plate spacing. In the radial case, the situation is a little different. Here, the magnetic force can increase *or* decrease adhesion during the initial stages of the pulling process. However, at some point all of the radial force curves will drop off as $1/L$, *much* less rapidly than in the nonmagnetic case. By choosing an appropriate ferrofluid (that is, by tuning M_0/H_0), one can presumably control when the force curves cross over from reducing adhesion to increasing adhesion.

Finally, observe that for a given b_0, the area below the gray solid curves in Fig. 6(a) [Fig. 6(b)] are considerably smaller (larger) than the corresponding area under the black dashed curves. This implies that the magnetic forces can reduce (enhance) the energy of separation as anticipated by the rigid case results depicted in Fig. 5. From Fig. 6 we conclude that both the peak adhesive force and the separation energy are significantly influenced by magnetic forces.

V. CONCLUSION

In this paper, we have shown that the introduction of a ferrofluid plus the action of an appropriate magnetic field configuration in a modified adhesion measurement system permits the adhesive strength to be opportunely controlled by magnetic means. Our analytical and numerical results show that the adhesive strength of a ferrofluid is reduced if the magnetic field is perpendicular to the plates or applied in-plane with azimuthal symmetry. Additionally, we have shown that the adhesive strength can be enhanced or reduced if the external field is in plane and pointing radially outward. So, having a bond strength adaptable to different applications, a magnetic fluid can perform different functions: it could either reduce adhesion when mechanical, nondestructive removal is needed, or increase adhesion when a high-shear strength, tough structural adhesive is necessary.

The ferrofluid thus acts as a sort of adjustable "magnetic glue," for which the adhesion strength is regulated by an applied magnetic field. This important and suggestive controlling mechanism is not only intrinsically interesting, but may allow the development of technological applications overlapping the fields of adhesion and ferrofluid research. Possible future applications may include the development of adhesive products in which adhesion could be switched on and off by a suitable magnetic field. In particular, removing

the adhesive force via a small hand-held magnet seems like a very useful possibility. Recent interesting studies have demonstrated that the adhesive properties of some solid/polymer interfaces can indeed be tuned by temperature [27,28]. The magnetically monitored adhesive process we present here would certainly add a welcome versatility to adhesion technology, even possibly allowing the emergence of a systematic way of controlling the reversibility of adherence using magnetic fields.

Our theoretical work makes specific predictions that have not yet been subjected to experimental check. It would be of interest to examine the relationship between adhesion and magnetic phenomena by performing probe-tack measurements with ferrofluids subjected to perpendicular, azimuthal, and in particular, radial magnetic field configurations [24,29,30]; these might even include such configurations as rotating [31–33] magnetic fields. A natural extension of the current work would be the investigation of the influence of magnetic forces on the adhesive properties of more complex magnetic fluids, such as magnetorheological suspensions [34], in which other important effects like elasticity, plasticity, shear thinning, and shear thickening could be monitored by external magnetic fields. In summary, we hope this work will instigate further theoretical and experimental studies on this rich topic.

ACKNOWLEDGMENTS

We thank the Brazilian Research Council/CNPq (J.A.M. and R.M.O.) and Dickinson College (D.P.J.) for financial support of this research. We gratefully acknowledge useful communications and stimulating discussions with Anke Lindner, Cyprien Gay, José Bico, Michael Widom, Raymond Goldstein, and Alexandre Rosas. We are greatly indebted to Andrejs Cebers for important discussions and useful suggestions.

APPENDIX: CALCULATION OF MAGNETIC FORCES USING AN ENERGY APPROACH

In this work, the magnetic effects were taken into account via a modified Darcy's law given by Eq. (1). This presupposes that one can write the magnetic forces in terms of a scalar potential Ψ_j. Indeed, the azimuthal and radial configurations both led to relatively simple scalar potentials and the magnetic forces could be calculated in closed form as shown in Eqs. (10) and (12). However, in the perpendicular configuration the scalar potential is a more complicated integral expression given by Eqs. (6) and (8) that leads to an even more complex expression for the force via Eq. (7). Because of the difficulties involved in calculating the forces in the perpendicular situation, we wondered whether there was an alternative method for calculating this force.

Because most of our difficulties involved integrating rather complicated expressions, it seemed appropriate to try to find the force using a differentiation process. Specifically, for a ferrofluid droplet whose magnetic energy is given as a function of height by $\mathcal{E}_m(b)$, the force exerted by the ferrofluid is given by

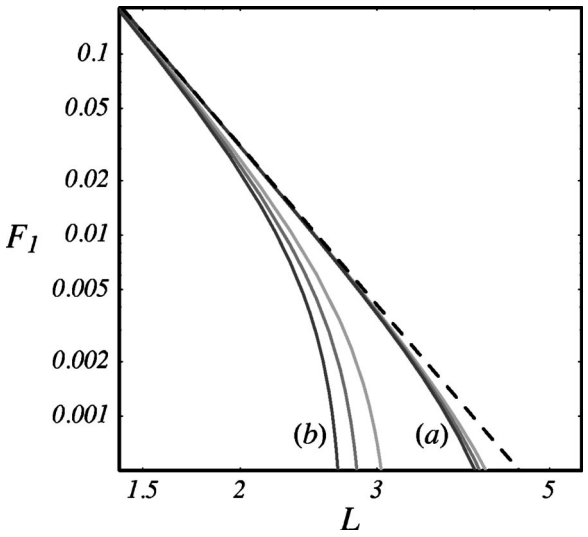

FIG. 7. Adhesion force for the perpendicular field configuration with the magnetic terms calculated via (a) the Darcy approach using Eq. (7), and (b) the energy approach using Eq. (A7). We have set $N_B^{\perp}=5.0\times10^{-3}$, $R_0=100$, and used the same initial plate spacings as before, $b_0=1.2$ (light gray), $b_0=1.7$ (medium gray), and $b_0=2.2$ (dark gray). The black dashed line shows the nonmagnetic situation.

$$F_m = -\frac{d\mathcal{E}_m}{db}. \tag{A1}$$

Now, the change in magnetic energy obtained by introducing a volume of magnetic fluid into a static magnetic field in free space is [11,12]

$$\mathcal{E}_m = -\frac{1}{2}\int \mathbf{M}\cdot\mathbf{B}_0 d\mathcal{V}, \tag{A2}$$

where $\mathbf{M}$ is the magnetization of the ferrofluid, $\mathbf{B}_0$ is the field that would be present in the absence of the ferrofluid, and the integration is taken over the volume of the ferrofluid $\mathcal{V}$. For example, in the azimuthal situation, we have a ferrofluid cylindrical annulus of height b and inner (outer) radius a (R). To be consistent with the approximations used in the Darcy approach, we assume the applied magnetic field given by $\mathbf{H}_a=(H_0a/r)\hat{\mathbf{e}}_\theta$ and magnetization given by $\mathbf{M}=(M_0a/r)\hat{\mathbf{e}}_\theta$. Equation (A2) then gives

$$\mathcal{E}_m^{\mathrm{azi}} = -\pi\mu_0 M_0 H_0 a^2 b \ln\left(\frac{R}{a}\right). \tag{A3}$$

Using volume conservation and performing the required differentiation, we obtain a magnetic force (scaled by $k\delta$) of

$$F_m^{\mathrm{azi}} = N_B^{\mathrm{azi}}\left\{\ln\left[1+(\gamma-1)\frac{b_0}{b}\right]-\frac{(\gamma-1)}{\dfrac{b}{b_0}+(\gamma-1)}\right\}, \tag{A4}$$

where γ and N_B^{azi} are as previously defined. Equation (A4) indicates an upward force and is exactly the same as the magnetic force given in Eq. (10) as expected. Note that the minus sign difference between Eq. (A4) and the correspond-

ing terms in Eq. (10) is due to our choice of coordinate system in describing the adhesion force.

Let us now try the same approach with the radial field configuration. In this case we have an applied field given by $\mathbf{H}_a=(H_0a/r)\hat{\mathbf{e}}_r$ and a magnetization given by $\mathbf{M}=(M_0a/r)\hat{\mathbf{e}}_r$. Carrying out the energy and force calculations, we find that the magnetic force in the radial case is exactly the same as in the azimuthal case given by Eq. (A4). At first this might seem strange since the radial and azimuthal magnetic fields point in different directions. However, since it is the *gradient* of the field magnitude that determines the force and the spatial dependence is identical in both situations, this should not be too surprising. What is surprising is the fact that in the radial situation, the magnetic force calculated from the energy as given by Eq. (A4) does not equal the magnetic force calculated from the Darcy approach as given in Eq. (12). The difference between the two approaches can be traced to the "surface" force term that comes from the boundary condition (3). This means that if we want to use the energy method, we must augment the force by inclusion of these surface terms. Specifically, Eq. (A1) should be replaced by

$$F_m = -\frac{d\mathcal{E}_m}{db} + \frac{1}{2}\mu_0 \int d\mathcal{A}[M_{jz}^2(r) - M_{jr}^2(R)]. \qquad \text{(A5)}$$

Here, as in Sec. II, the integration is taken over the cross sectional area $\mathcal{A}$ of the ferrofluid surface in contact with the upper plate.

Although Eq. (A5) is not quite as simple as Eq. (A1), it is still potentially much easier to use in some situations than Eq. (5). As an example, let us now consider the perpendicular field configuration. In this case, the ferrofluid droplet is in the shape of a cylinder of height b and radius R. The energy of this configuration, is, apart from a constant term proportional to the volume, given by [14,15]

$$\mathcal{E}_m^{\perp} = \frac{4}{3}\mu_0 M^2 R^3 \{1 - q^{-3}[(2q^2-1)E(q) + (1-q^2)K(q)]\}, \qquad \text{(A6)}$$

where K and E are, respectively, complete elliptic integrals of the first and second kind, and $q^2=\zeta^2/(1+\zeta^2)$ (recall that $\zeta=2R/b$). Again, using volume conservation and performing the differentiation, Eq. (A5) gives a dimensionless force of

$$F_m^{\perp} = N_B^{\perp}\left(\frac{b_0}{b}\right)\left\{\frac{q^3 - (2-q^2)E(q) + 2(1-q^2)K(q)}{q^2\sqrt{1-q^2}} + \frac{\pi}{2}\right\}, \qquad \text{(A7)}$$

where $N_B^{\perp}$ is defined as before.

Equation (A7) gives a closed form expression for the magnetic contribution to the adhesion force in the perpendicular field configuration. But this information is supposedly contained in Eq. (7) as well. Figure 7 shows the adhesion force as calculated using both (a) the Darcy approach and (b) the energy approach. Although qualititatively similar, these two forces are clearly *not* the same. The energy approach shows a dramatically decreased adhesion force. But why? It turns out that when using the Darcy approximation in the perpendicular field configuration, one uses only the lowest nonvanishing component of the magnetic field [16], whereas in the energy calculation, the entire demagnetizing field is taken into account. Thus it seems as though the energy approach in this case should provide a more accurate approximation to the magnetic force. Additionally, the energy approach gives a closed form expression for the magnetic force and is therefore much simpler to use in calculations.

We find it a bit surprising that there is such a large difference between the Darcy approach and the energy approach in the perpendicular configuration. This suggests that the radial component of the demagnetizing field may play an important role in determining the evolution of a ferrofluid drop. Of course, the results reported in Ref. [16] show excellent agreement with experiments suggesting that the radial component is not a relevant factor in determining the final state patterns. Clearly, this is an unresolved issue. It would be very interesting to know exactly what role (if any) the radial component plays in these ferrofluid evolutions.

[1] C. Gay and L. Leibler, Phys. Today **52**(11), 48 (1999).
[2] D. W. Aubrey, *Aspects of Adhesion*, edited by K. W. Allen (Elsevier, New York, 1988).
[3] D. J. Yarusso, *Adhesion Science and Engineering—The Mechanics of Adhesion*, edited by D. A. Dillard and A. V. Pocius (Elsevier, Amsterdam, 2002).
[4] A. Zosel, Colloid Polym. Sci. **263**, 541 (1985).
[5] H. Lakrout, P. Sergot, and C. Creton, J. Adhes. **69**, 307 (1999).
[6] B. A. Francis and R. G. Horn, J. Appl. Phys. **89**, 4167 (2001).
[7] S. Poivet, F. Nallet, C. Gay, and P. Fabre, Europhys. Lett. **62**, 244 (2003).
[8] D. Derks, A. Lindner, C. Creton, and D. Bonn, J. Appl. Phys. **93**, 1557 (2003).
[9] M. Tirumkudulu, W. B. Russel, and T. J. Huang, Phys. Fluids **15**, 1588 (2003).
[10] J. A. Miranda, Phys. Rev. E **69**, 016311 (2004).
[11] R. E. Rosensweig, *Ferrohydrodynamics* (Cambridge University Press, Cambridge, England, 1985), and references therein.
[12] E. Blums, A. Cebers, and M. M. Maiorov, *Magnetic Fluids* (de Gruyter, New York, 1997), and references therein.
[13] P. G. Saffman and G. I. Taylor, Proc. R. Soc. London, Ser. A **245**, 312 (1958).
[14] A. O. Tsebers and M. M. Maiorov, Magnetohydrodynamics (N.Y.) **16**, 21 (1980).
[15] S. A. Langer, R. E. Goldstein, and D. P. Jackson, Phys. Rev. A **46**, 4894 (1992).

[16] D. P. Jackson, R. E. Goldstein, and A. O. Cebers, Phys. Rev. E **50**, 298 (1994).
[17] G. Pacitto, C. Flament, J.-C. Bacri, and M. Widom, Phys. Rev. E **62**, 7941 (2000).
[18] C. Flament, S. Lacis, J.-C. Bacri, A. Cebers, S. Neveu, and R. Perzynski, Phys. Rev. E **53**, 4801 (1996).
[19] M. Zahn and R. E. Rosensweig, IEEE Trans. Magn. **16**, 275 (1980).
[20] J. A. Miranda, Phys. Rev. E **62**, 2985 (2000).
[21] D. P. Jackson and J. A. Miranda, Phys. Rev. E **67**, 017301 (2003).
[22] A. O. Cebers, Magnetohydrodynamics (N.Y.) **17**, 113 (1981).
[23] A. O. Cebers, Magnetohydrodynamics (N.Y.) **21**, 142 (1985).
[24] W. H. Heiser and J. A. Shercliff, J. Fluid Mech. **22**, 701 (1965).
[25] P. Ramamoorthy, Phys. Fluids **4**, 1444 (1961).
[26] S. Y. Molokov and J. E. Allen, J. Phys. D **25**, 393 (1992).
[27] G. de Crevoisier, P. Fabre, J.-M. Corpart, and L. Leibler, Science **285**, 1246 (1999).
[28] S. Khongtong and G. S. Ferguson, J. Am. Chem. Soc. **124**, 7254 (2002).
[29] D. R. Ohlsen and P. B. Rhines, J. Fluid Mech. **338**, 35 (1997).
[30] R. E. Rosensweig, J. Browaeys, J.-C. Bacri, A. Zebib, and R. Perzynski, Phys. Rev. Lett. **83**, 4904 (1999).
[31] J.-C. Bacri, A. O. Cebers, and R. Perzynski, Phys. Rev. Lett. **72**, 2705 (1994).
[32] A. Cebers, Phys. Rev. E **66**, 061402 (2002).
[33] C. Lorenz and M. Zahn, Phys. Fluids **15**, S4 (2003).
[34] See, for instance, A. Kawai *et al.* in *Proceedings of the Eighth International Conference on Electro-Rheological and Magneto-Rheological Suspensions*, edited by G. Bossis (World Scientific, Singapore, 2002).